Analytical and Bioanalytical Chemistry
https://doi.org/10.1007/s00216-024-05538-9

PAPER IN FOREFRONT

A shifted ratio spectrum strategy for effective subtraction of fluorescence interference in Raman spectra

Zhiqiang Wang[1] · Siwen Ju[1] · Xiaofei Zhou[2] · Feng Ni[3] · Yanhua Qiu[2] · Ruiting Zhang[1] · Lin Ma[1] · Ke Lin[1]

Received: 1 August 2024 / Revised: 4 September 2024 / Accepted: 9 September 2024

Abstract

Raman spectroscopy is an important technique for analyzing the chemical composition of samples in many fields. A severe challenge often encountered in Raman measurements is the presence of a concurrent fluorescence background, especially in biological samples. In order to obtain accurate Raman spectra, the fluorescence background must be subtracted from the original Raman spectra. We proposed a shifted ratio spectrum method to subtract the strong fluorescence background from the original Raman spectrum. First, the original Raman spectrum is divided into multiple regions according to the spectral shape of the shifted ratio spectra, and then, Gaussian fitting is performed in each region. The fitting results are stitched together in order to obtain the complete fluorescence background. Finally, this fluorescence background is subtracted from the original spectrum to obtain a pure Raman spectrum. This method can accurately subtract the fluorescence background of Rhodamine 6G (R6G)/ethanol solution and serum. This highlights the great potential of this method for applications in both biological and non-biological samples.

Keywords Raman spectra · Serum · Fluorescence background · Shifted ratio spectra · Gaussian fitting

Introduction

To date, Raman spectroscopy has developed into a useful and powerful spectral analysis technique that can quickly and non-destructively identify the composition and microstructure of a sample. This technology has great application potential, such as disease diagnosis [1–6], food safety testing [7, 8], mineral analysis [9, 10], explosives detection [11, 12], cultural relic identification [13], and quality control [14, 15]. A serious challenge often encountered in Raman measurements is the presence of a concurrent fluorescence background. Fluorescence often affects the detection of Raman signals because the fluorescence intensity is usually several orders of magnitude larger than the Raman scattering signal, especially in biological samples. For example, in human serum [16, 17], skin [18], and most drugs [19], some low-concentration impurities with large fluorescence yields are often difficult to remove. Even weak fluorescence with a quantum yield of about 10^{-4} can mask the Raman signal with a quantum yield of about 10^{-7}. Strong fluorescence interference limits the application of Raman spectroscopy. Therefore, in order to obtain an accurate Raman spectrum of the sample, its fluorescence interference needs to be subtracted from the original Raman spectrum.

A variety of methods have been developed to remove the fluorescence background, which can be divided into three types. The first type is based on sample pretreatment. For example, filtering [16] or photobleaching [18, 20] the sample before acquiring the Raman spectrum can effectively reduce the fluorescence background. However, pretreatment may change the composition and structure of the sample.

The second type is based on the difference between the intrinsic properties of Raman signals and fluorescence. For example, Raman signals precede fluorescence radiation, so the fluorescence signal can be reduced by using ultrashort laser pulses, intensified charge-coupled devices (ICCD), Kellman devices, and other time-resolved devices [19, 21]. The polarization characteristics of Raman signals and fluorescence are also different. Two spectra can be obtained

✉ Ke Lin
klin@xidian.edu.cn

[1] School of Physics, Xidian University, Xi'an 710071, P. R. China

[2] The Affiliated Hospital of Xidian University, Xi'an 710071, P. R. China

[3] The Third Affiliated Hospital of Xi'an Medical University, Xi'an 710000, P. R. China

Published online: 18 September 2024

using parallel and perpendicular polarized excitation light. Subtracting these two spectra can also remove a certain amount of the fluorescence background [22]. The sources of Raman signals and fluorescence are also different. Usually, fluorescence is generated only when the wavelength of the laser matches the molecular energy level. Many samples have weak absorption of infrared and ultraviolet light. Therefore, using infrared or ultraviolet light as an excitation light can effectively suppress fluorescence [23, 24]. In addition, fluorescence has another characteristic: when the wavelength of the excitation light shifts slightly, the Raman signal will also shift slightly accordingly, while the fluorescence background will hardly change. Based on this characteristic, the shifted excitation Raman difference spectroscopy (SERDS) method was proposed [25–29]. This method requires the use of light sources with different wavelengths that are very close to each other as excitation light, which can also remove the fluorescence background. However, the above methods all require the design and modification of the instruments, and the instruments involved may be complex and expensive, so it is difficult to promote them on many devices.

Different from the previous two methods, the third type is to process the original Raman spectrum, such as frequency domain filtering [16, 30], wavelet transformation [31, 32], and polynomial fitting [33–35]. Among them, the use of polynomial fitting to subtract fluorescence background has been more commonly used in recent years. However, the above data processing methods may produce some artifacts or overfitting, which may cause errors when discussing spectral details.

Recently, we proposed a Raman ratio spectrum method and successfully used it to extract weak Raman bands that heavily overlap with strong bands [36, 37]. We also extracted weak Raman spectra of hydration shells in aqueous solution to infer the microstructure of the hydration shells [38–40]. Inspired by this, we further proposed a data processing method for a shifted ratio spectrum method to subtract the fluorescence background in the Raman spectrum. This method can accurately subtract the fluorescence background in Rhodamine 6G (R6G)/ethanol solution and serum.

Experimental details

R6G (> 99.0%) and C_2H_5OH (> 99.7%) were purchased from Sinopharm Chemical Reagent Co., Ltd. The R6G/ethanol solutions were prepared by weight. The serum samples were provided by the Affiliated Hospital of Xidian University and came from a healthy volunteer. The solutions were held in a SiO_2 cuboid cell (1 cm × 1 cm × 3 cm).

The experiments were conducted using a spontaneous Raman spectrometer equipped with a continuous laser (coherent, GenesisMX532-1000, 532 nm), a three-stage monochromator (Beijing Zhuoli Hanguang Instrument Co., Ltd., Omni λ-180D and Omni λ-5008i), and an electrically cooled CCD (Andor, DR-316B-LDC-DD), as described in detail previously [41]. The Raman spectra were measured in a back-scattering geometry with a spectral resolution of approximately 2.0 cm^{-1}. The polarization of the laser was controlled using a Glan-Taylor prism and a half-wave plate. The polarization of the excitation light and the collected Raman scattering are in the same direction. The laser power used for R6G/ethanol solution is 120 mW and the exposure time is 12 s. The laser power used for serum is 250 mW and the exposure time is 60 s. The CCD was cooled to − 60 °C during the experiment.

Results and discussion

Principle of shifted ratio spectra

The proposed shifted ratio spectrum is a method to subtract the fluorescence background from the Raman spectrum by mathematical processing. Since the fluorescence peak is usually broad, a segment of the fluorescence spectrum can be fitted using a Gaussian peak. Here, it is assumed that an original fluorescence peak can be expressed by the following equation:

$$I(\lambda) = Ae^{-\left(\frac{\lambda-\lambda_0}{\omega}\right)^2} \tag{1}$$

A is the maximum intensity, λ_0 is the center position of the Gaussian peak, and ω controls the width of the spectrum. Move the center position by $\Delta\lambda$ nm, and the shifted fluorescence spectrum can be written as the following equation. The principle is to make $\Delta\lambda$ as small as possible while clearly highlighting the spectral characteristics, about one order of magnitude smaller than the peak width.

$$I'(\lambda) = Ae^{-\left(\frac{\lambda-\lambda_0-\Delta\lambda}{\omega}\right)^2} \tag{2}$$

Dividing the original spectrum $I(\lambda)$ by the shifted spectrum $I'(\lambda)$, the shifted ratio spectrum $R(\lambda)$ is obtained, as shown in the following equation:

$$R(\lambda) = \frac{I(\lambda)}{I\prime(\lambda)} \tag{3}$$

Then, plugging Eqs. (1) and (2) into Eq. (3), the shifted ratio spectrum $R(\lambda)$ can be written as the following equation:

$$R(\lambda) = e^{\frac{(2\lambda_0+\Delta\lambda)\Delta\lambda}{\omega^2}} e^{-\frac{2\Delta\lambda\lambda}{\omega^2}} \tag{4}$$

The first term in the above Eq. (4) is a constant. For a fluorescence peak, its width ω is usually relatively large, and $\Delta\lambda$ is a small value selected artificially, so the

exponent of the second term $2\Delta\lambda\lambda/\omega^2$ tends to be infinitesimal. The second term can be approximately expanded using the first-order Taylor formula as follows:

$$e^{-\frac{2\Delta\lambda\lambda}{\omega^2}} \approx 1 - \frac{2\Delta\lambda\lambda}{\omega^2} \tag{5}$$

Plugging Eq. (5) into Eq. (4), the shifted ratio spectrum $R(\lambda)$ can be simplified to a linear equation as follows:

$$R(\lambda) = k\lambda + b \tag{6}$$

$$k = -e^{\frac{(2\lambda_0+\Delta\lambda)\Delta\lambda}{\omega^2}} \frac{2\Delta\lambda}{\omega^2} \tag{7}$$

$$b = e^{\frac{(2\lambda_0+\Delta\lambda)\Delta\lambda}{\omega^2}} \tag{8}$$

For example, the black solid line in Fig. 1a is a simulated original fluorescence spectrum $I(\lambda)$ ($\lambda_0 = 567$ nm, $\omega = 30$), and the red dotted line is the shifted fluorescence spectrum $I'(\lambda)$ ($\Delta\lambda = 0.5$ nm). $I(\lambda)$ divided by $I'(\lambda)$ gives the shifted ratio spectrum $R(\lambda)$, as shown by the pink solid line in Fig. 1b, which can be well fitted with a straight line, as shown by the blue dotted line. The above analysis should also be true in reverse, that is, if the shifted ratio spectrum $R(\lambda)$ can be fitted with a straight line within a certain wavelength range, then the fluorescence spectrum within this range can also be well fitted with a Gaussian peak.

In order to verify the correctness of the above analysis, we measured the fluorescence spectrum of R6G/ethanol solution. R6G is an organic laser dye with a high fluorescence quantum yield and is often used as a fluorescence probe molecule [42, 43]. As shown in Fig. 1c, the black solid line is the fluorescence spectrum of R6G/ethanol solution with a concentration of 0.0167 mM, and the red dotted line is the shifted spectrum ($\Delta\lambda = 0.2$ nm) which is obtained by shifting the spectrum to the low wavelength direction by 0.2 nm. The corresponding shifted ratio spectrum $R(\lambda)$ is shown as the pink solid line in Fig. 1d. $R(\lambda)$ is a curve instead of a straight line because the fluorescence spectrum of R6G is not a simple Gaussian distribution. However, we noticed that if the shifted ratio spectrum $R(\lambda)$ is divided into several regions (vertical grayscale stripes), a straight line can be approximately fitted in each region, as shown in Fig. 1d (blue dotted line). So, the original fluorescence spectrum can also be fitted with a Gaussian peak in each divided area. The more region $R(\lambda)$ is divided into, the smaller the fitting error is, but the amount of calculation will increase. Usually, the regions can be selected by observing the shape of the shifted ratio spectrum $R(\lambda)$.

The fluorescence spectrum of the above R6G/ethanol solution (Fig. 2a, black solid line) was divided into six

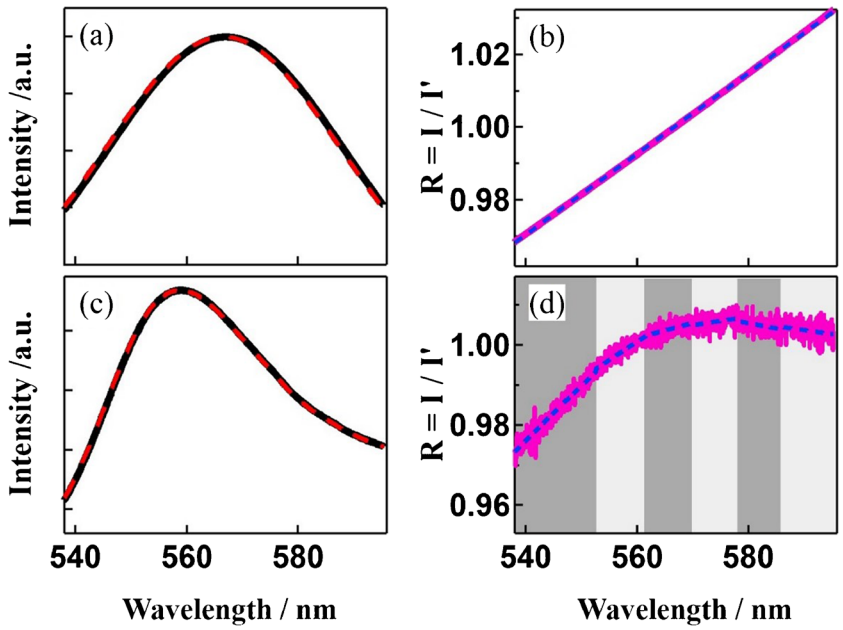

Fig. 1 **a** The simulated original fluorescence spectrum $I(\lambda)$ ($\lambda_0 = 567$ nm, $\omega = 30$, black solid line) and the shifted fluorescence spectrum $I'(\lambda)$ ($\Delta\lambda = 0.5$ nm, red dotted line). **b** The obtained shifted ratio spectrum $R(\lambda)$ (pink solid line), which can be well fitted by a straight line (blue dotted line). **c** The fluorescence spectrum of R6G/ethanol solution with the concentration of 0.0167 mM (black solid line), and the shifted fluorescence spectrum (red dotted line, $\Delta\lambda = 0.2$ nm). **d** The obtained shifted ratio spectrum $R(\lambda)$ of R6G/ethanol solution (pink solid line), and the results of piecewise linear fitting (blue dotted line). The vertical gray stripes are the 6 regions divided by shifted ratio spectra

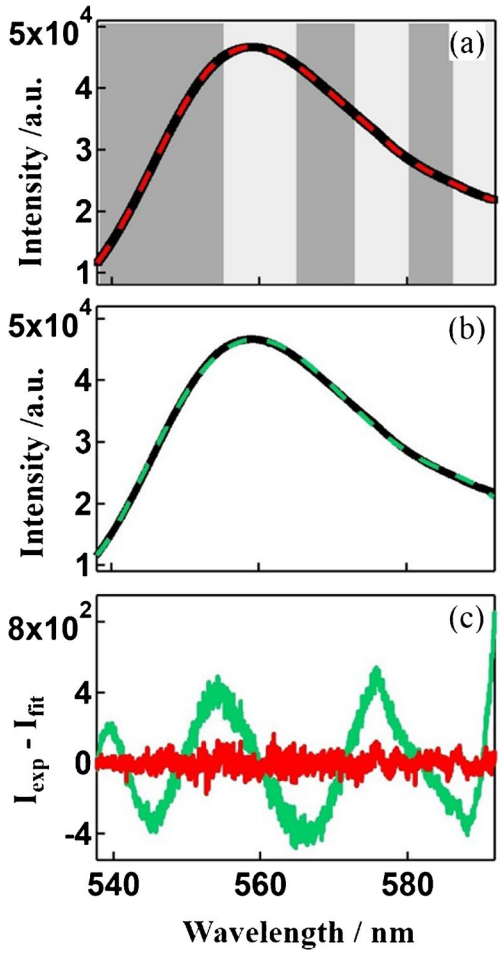

Fig. 2 **a** The black solid line is the fluorescence spectrum of R6G/ethanol solution with a concentration of 0.0167 mM, the red dotted line is the results of the fitting by piecewise Gaussian fitting, and the vertical gray stripes are the 6 regions divided by shifted ratio spectra. **b** The black solid line is the fluorescence spectrum of R6G/ethanol solution with a concentration of 0.0167 mM and the green dotted line is the results of the fitting by a sixth-order polynomial. **c** The red line is the differential spectrum of panel (**a**) and the green line is the differential spectrum of panel (**b**)

regions and fitted with Gaussian peaks. The fitting result is shown in the red dotted line of Fig. 2a. The process of regional fitting is shown in Fig. S1 (as seen in Supporting Information). In order to highlight the accuracy of this method, the polynomial fitting method widely used in the literature was also applied to fit the original fluorescence spectrum, and the results are shown in Fig. 2b (green dotted line). The sixth-order polynomial fitting function used in Fig. 2b is shown in Equation S1 (as seen in Supporting Information). The literature usually uses fourth- to sixth-order polynomials for fitting [44–46], so we use a sixth-order polynomial for fitting here. The fitting results of the two methods can be compared by the difference spectrum between the fitting spectrum and the original spectrum, as shown in Fig. 2c. From the results, it can be seen that the error of the piecewise Gaussian fitting (red line) is significantly smaller than that of the polynomial fitting (green line). Therefore, the shifted ratio spectrum method we proposed here can fit the fluorescence spectrum more accurately, and we can use this method to eliminate the fluorescence background in Raman spectra.

Fluorescence components subtraction in Raman spectrum of R6G/ethanol solution

In order to verify whether the shifted ratio spectrum method can be used to remove the fluorescence background in the Raman spectrum, the Raman spectrum of R6G/ethanol solution was measured, as shown in Fig. 3a (black solid line). By comparison, in the Raman spectrum of Fig. 3a, the shape of the fluorescence background is different from that in the fluorescence spectrum of Fig. 2a. This is because the concentration of the solution here is different from before. This solution was prepared by continuously diluting the concentration of R6G until the Raman signal of ethanol could be weakly observed against a strong fluorescence background. The fluorescence spectrum of R6G will change with its concentration [47], but these do not affect the use of this method.

In the measured spectrum, the Raman signal of ethanol is very weak, almost being overwhelmed by the strong fluorescence signal of R6G. Therefore, the Raman signal of ethanol is difficult to obtain directly from the original spectrum. The shifted Raman spectrum (Fig. 3a, red dotted line) was obtained by shifting the original Raman spectrum toward low wavenumbers by 4.1 cm^{-1}. And then, the shifted ratio spectrum $R(\lambda)$ (Fig. 3b) was obtained by dividing the original Raman spectrum by the shifted Raman spectrum. In the shifted ratio spectrum, it can be clearly observed that there are at least five spectral peaks, corresponding to the Raman signal of ethanol, and the star symbols are used to mark the peaks in Fig. 3b. This indicates that the Raman signal of ethanol, which is very weak in the original spectrum, can be amplified in the shifted ratio spectrum.

The entire original spectrum is appropriately divided into multiple regions according to the linearity of the shifted ratio spectrum. The principle of division is that in each small area, the shifted ratio spectrum can be linearly fitted. In this way, the fluorescence background of the original spectrum in the corresponding region can be fitted by a Gaussian peak. The pure Raman spectrum is obtained by subtracting the corresponding fluorescence background from the original spectrum. The same operation is performed in each area and then spliced to obtain a Raman spectrum without the fluorescence background. It should be noted that before fitting the spectrum of each region, the band with the Raman signal must be deleted first. This can reduce the fitting error. The

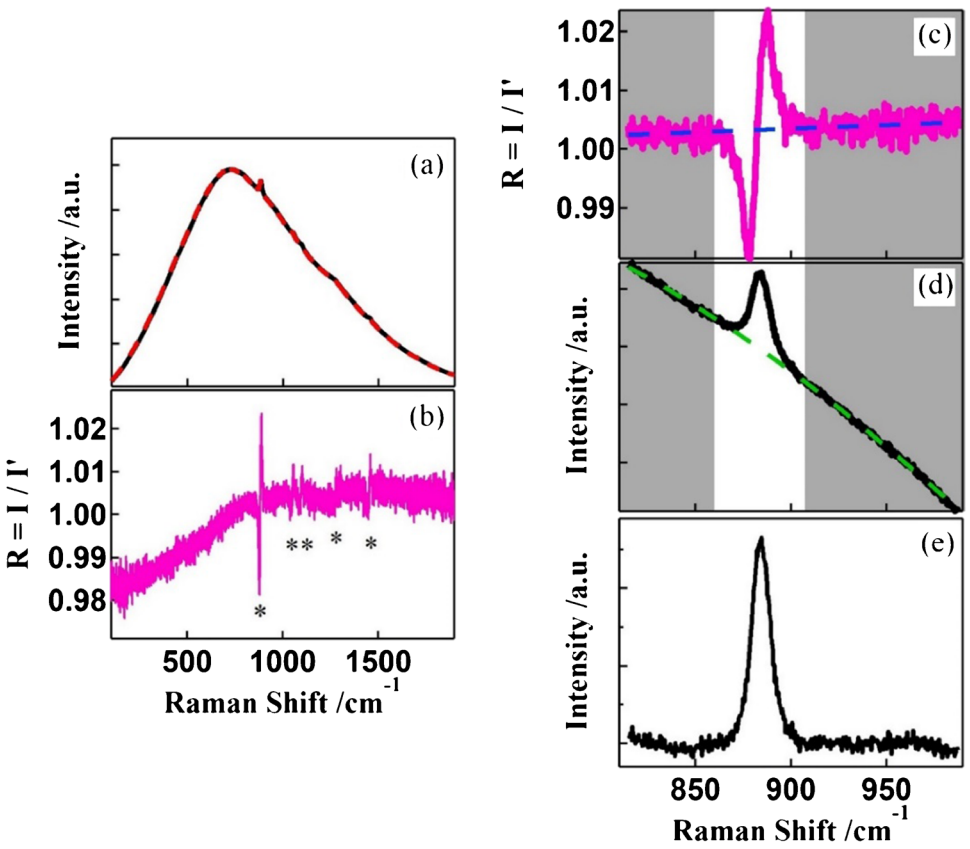

Fig. 3 **a** The black solid line is the original Raman spectrum of R6G/ethanol solution and the red dotted line is the shifted spectrum, $\Delta\nu = 4.1\ cm^{-1}$. **b** The shifted ratio spectrum $R(\nu)$ of R6G/ethanol solution. **c** The pink solid line is a part of the shifted ratio spectrum in the range 820 ~ 990 cm^{-1} taken from panel (**b**) and the blue dotted line is the result of linear fitting after ignoring the Raman signal from the spectrum. **d** The black solid line is a part of the original Raman spectrum in the range 820 ~ 990 cm^{-1} taken from panel (**a**), the green dotted line is the result of Gaussian fitting after ignoring the Raman signal from the spectrum, and the vertical gray bands are the fluorescence background range on which the fitting depends. **e** The Raman spectrum of ethanol obtained by subtracting the fluorescence background

specific range of the deleted band can be selected by observing the shifted ratio spectrum.

Taking the spectral range of 820 ~ 990 cm^{-1} as an example, it can be seen from Fig. 3c that when the Raman signal is ignored, the shifted ratio spectrum (pink solid line) in this region can be well linearly fitted (blue dotted line). So, in this region, the fluorescence background of the original spectrum can be fitted by a Gaussian peak in Fig. 3d (green dotted line). The pure Raman spectrum of ethanol can be obtained by subtracting the fitted fluorescence background from the original spectrum in this region, as shown in Fig. 3e.

The entire original spectrum was divided into several spectral regions, and the fluorescence background of each region was removed one by one, and then spliced it together to obtain the complete pure Raman spectrum of ethanol, as shown in Fig. 4a. The Raman characteristic peaks of ethanol were clearly observed at 443, 881, 1048, 1093, 1274, and 1453 cm^{-1} [48, 49]. This result is significantly better than that before subtracting the fluorescence background (Fig. 3a). Therefore, it can be seen from the results in Fig. 4 that the Raman spectrum of ethanol obtained after subtracting the fluorescence background is basically the same as the Raman spectrum of pure ethanol, except that the signal-to-noise ratio is slightly reduced. This shows that the shifted ratio spectrum method can indeed effectively remove the fluorescence background in the Raman spectrum. In actual measurements, we can improve the signal-to-noise ratio by increasing the excitation light intensity, integration time, and number of repeated measurements when collecting the Raman spectrum.

Fluorescence interference subtraction in Raman spectrum of biological sample

The shifted ratio spectrum method of removing fluorescence interference can be used not only in the R6G/ethanol system, but also in biological samples such as blood. The content of blood components has always been an important basis for doctors to control drug dosage, analyze the interaction between pathogens and drugs, and track the recovery of patients. In addition, Raman spectroscopy analysis of human blood has been used in the detection of many pathogens [50, 51]. However, there is strong fluorescence interference in the Raman spectrum of blood, which will affect the analysis of the Raman spectrum, so the fluorescence interference needs to be subtracted. Next, we will use the shifted ratio spectrum method to subtract the fluorescence background from the Raman spectrum of human blood.

The Raman spectrum of human serum was measured, as shown in Fig. 5a (black solid line), which is accompanied by a strong fluorescence background. Here, we shift the original

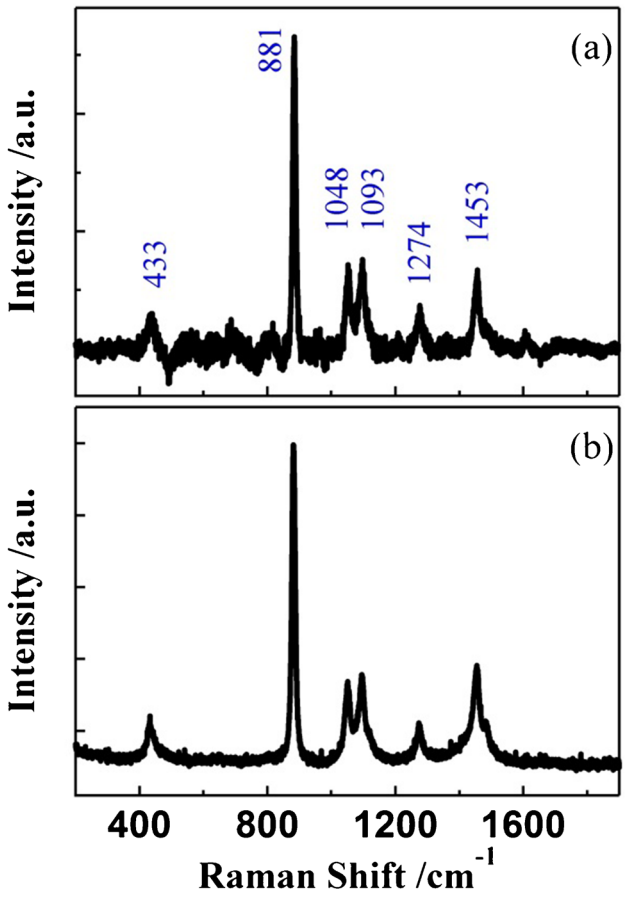

Fig. 4 Raman spectrum of R6G/ethanol solution after removing fluorescence background (**a**) and Raman spectrum of pure ethanol (**b**)

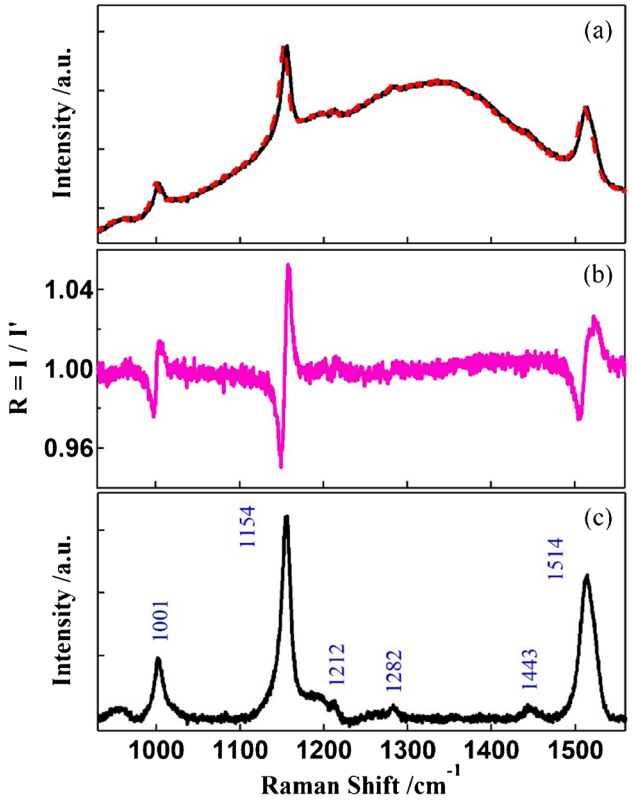

Fig. 5 **a** The black solid line is the original Raman spectrum of the human serum and the red dotted line is the shifted spectrum, $\Delta\nu = 3.2$ cm^{-1}. **b** The shifted ratio spectrum obtained by dividing the original Raman spectrum by the shifted spectrum. **c** The Raman spectrum of the human serum obtained by subtracting the fitted fluorescence background

spectrum to a low wavenumber by 3.2 cm^{-1} to obtain the shifted spectrum (red dotted line). The original spectrum was then divided by the shifted spectrum to obtain the shifted ratio spectrum (Fig. 5b). By regional fitting and subtracting the fluorescence background, the Raman spectrum of serum can be obtained (Fig. 5c). The Raman peaks at 1001 cm^{-1}, 1154 cm^{-1}, and 1514 cm^{-1} can be clearly observed, which may be attributed to C-C stretching vibration of the aromatic ring and the C-C (and C-N) stretching vibration and the C=C stretching vibration of carotene in serum [16, 52]. In addition to these three obvious peaks, several other peaks with extremely small intensities can also be obtained, located at 1212 cm^{-1}, 1282 cm^{-1}, and 1443 cm^{-1}. These three peaks are almost unobservable in the original spectrum.

Conclusions

In summary, in order to obtain accurate Raman spectra, the fluorescence background must be subtracted from the original Raman spectra. We proposed a shifted ratio spectrum method to subtract the strong fluorescence background from the original Raman spectrum. First, the original Raman spectrum is divided into multiple regions according to the spectral shape of the shifted ratio spectrum, and then, Gaussian fitting is performed in each region. The fitting results are stitched together in order to obtain the complete fluorescence background. Finally, this fluorescence background is subtracted from the original spectrum to obtain a pure Raman spectrum. This method can accurately subtract the fluorescence background of Rhodamine 6G (R6G)/ethanol solution and serum. This method has great potential in biological and non-biological sample applications.

Supplementary Information The online version contains supplementary material available at https://doi.org/10.1007/s00216-024-05538-9.

Author contribution Conceptualization: Zhiqiang Wang, Ke Lin. Methodology: Zhiqiang Wang, Ke Lin. Formal analysis and investigation: Zhiqiang Wang, Siwen Ju, Xiaofei Zhou, Feng Ni, Yanhua Qiu, Ruiting Zhang, Lin Ma, Ke Lin. Writing — original draft preparation: Zhiqiang Wang, Siwen Ju. Writing — revise and editing: Zhiqiang Wang, Ke Lin.

Funding This work was supported by the Key Research Project of Shaanxi Provincial Science and Technology Department (2023-YBNY-158); the Xi'an Science and Technology Project (22NYYF016); the Natural Science Foundation of Shaanxi Province (2022JM-087); the Open Fund of the State Key Laboratory of Molecular Reaction Dynamics in DICP, CAS, (SKLMRD-K202413); and the 111 Project.

Declarations

Ethics approval The project has passed the review of the ethics committee.

Source of biological material The serum samples were provided by the Affiliated Hospital of Xidian University and came from a healthy volunteer.

Competing interests The authors declare no competing interests.

References

1. Huang L, Sun H, Sun L, Shi K, Chen Y, Ren X, Ge Y, Jiang D, Liu X, Knoll W, Zhang Q, Wang Y. Rapid, label-free histopathological diagnosis of liver cancer based on Raman spectroscopy and deep learning. Nat Commun. 2023;14(1). https://doi.org/10.1038/s41467-022-35696-2.
2. Abramczyk H, Brozek-Pluska B. Raman imaging in biochemical and biomedical applications. Diagnosis and treatment of breast cancer. Chem Rev. 2013;113(8):5766–81. https://doi.org/10.1021/cr300147r.
3. Wang Z, Lin W, Luo C, Xue H, Wang T, Hu J, Huang Z, Fu D. Early diagnosis of thyroid-associated ophthalmopathy using label-free Raman spectroscopy and multivariate analysis. Spectrochim Acta A Mol Biomol Spectrosc. 2024;310. https://doi.org/10.1016/j.saa.2024.123905.
4. Chang C, Liu H, Chen C, Wu L, Lv X, Xie X, Chen C. Rapid diagnosis of systemic lupus erythematosus by Raman spectroscopy combined with spiking neural network. Spectrochim Acta A Mol Biomol Spectrosc. 2024;310. https://doi.org/10.1016/j.saa.2024.123904.
5. Zhang C, Tan JB, Du BQ, Ji C, Pei ZY, Shao MR, Jiang SZ, Zhao XF, Yu J, Man BY, Li Z, Xu KC. Reversible thermoelectric regulation of electromagnetic and chemical enhancement for rapid SERS detection. ACS Appl Mater Interfaces. 2024;16(9):12085–94. https://doi.org/10.1021/acsami.3c18409.
6. Liu YH, Qiao SD, Fang C, He Y, Sun HY, Liu J, Ma YF. A highly sensitive LITES sensor based on a multi-pass cell with dense spot pattern and a novel quartz tuning fork with low frequency. Opto-Electron Adv. 2024;7(3):230230-230230. ARTN 230230. https://doi.org/10.29026/oea.2024.230230.
7. Nilghaz A, Mahdi Mousavi S, Amiri A, Tian J, Cao R, Wang X. Surface-enhanced Raman spectroscopy substrates for food safety and quality analysis. J Agric Food Chem. 2022;70(18):5463–76. https://doi.org/10.1021/acs.jafc.2c00089.
8. Zou M-Q, Zhang X-F, Qi X-H, Ma H-L, Dong Y, Liu C-W, Guo X, Wang H. Rapid authentication of olive oil adulteration by Raman spectrometry. J Agric Food Chem. 2009;57(14):6001–6. https://doi.org/10.1021/jf900217s.
9. Sharma SK, Porter JN, Misra AK, Acosta-Maeda TE, Angel SM, McKay CP. Standoff Raman spectroscopy for future Europa Lander missions. J Raman Spectrosc. 2020;51(9):1782–93. https://doi.org/10.1002/jrs.5814.
10. Wang Y, Xiao J, Zhu H, Li Y, Alsaid Y, Fong KY, Zhou Y, Wang S, Shi W, Wang Y, Zettl A, Reed EJ, Zhang X. Structural phase transition in monolayer MoTe2 driven by electrostatic doping. Nature. 2017;550(7677):487–91. https://doi.org/10.1038/nature24043.
11. Carroll JA, Izake EL, Cletus B, Jaatinen E. Eye-safe UV standoff Raman spectroscopy for the ranged detection of explosives in the field. J Raman Spectrosc. 2015;46(3):333–8. https://doi.org/10.1002/jrs.4642.
12. Hao R, Zhao J, Liu J, You H, Fang J. Remote Raman detection of trace explosives by laser beam focusing and plasmonic spray enhancement methods. Anal Chem. 2022;94(32):11230–7. https://doi.org/10.1021/acs.analchem.2c01732.
13. Wang X, Zhen G, Hao X, Tong T, Ni F, Wang Z, Jia J, Li L, Tong H. Spectroscopic investigation and comprehensive analysis of the polychrome clay sculpture of Hua Yan Temple of the Liao Dynasty. Spectrochim Acta A Mol Biomol Spectrosc. 2020;240. https://doi.org/10.1016/j.saa.2020.118574.
14. Li W, Wu S, Zhang H, Zhang X, Zhuang J, Hu C, Liu Y, Lei B, Ma L, Wang X. Enhanced biological photosynthetic efficiency using light-harvesting engineering with dual-emissive carbon dots. Adv Funct Mater. 2018;28(44). https://doi.org/10.1002/adfm.201804004.
15. Esmonde-White KA, Cuellar M, Lewis IR. The role of Raman spectroscopy in biopharmaceuticals from development to manufacturing. Anal Bioanal Chem. 2021;414(2):969–91. https://doi.org/10.1007/s00216-021-03727-4.
16. Tatarkovic M, Synytsya A, Stovickova L, Bunganic B, Miskovicová M, Petruzelka L, Setnicka V. The minimizing of fluorescence background in Raman optical activity and Raman spectra of human blood plasma. Anal Bioanal Chem. 2015;407(5):1335–42. https://doi.org/10.1007/s00216-014-8358-7.
17. Bahreini M, Hosseinzadegan A, Rashidi A, Miri SR, Mirzaei HR, Hajian P. A Raman-based serum constituents' analysis for gastric cancer diagnosis: in vitro study. Talanta. 2019;204:826–32. https://doi.org/10.1016/j.talanta.2019.06.068.
18. Bonnier F, Ali SM, Knief P, Lambkin H, Flynn K, McDonagh V, Healy C, Lee TC, Lyng FM, Byrne HJ. Analysis of human skin tissue by Raman microspectroscopy: dealing with the background. Vib Spectrosc. 2012;61:124–32. https://doi.org/10.1016/j.vibspec.2012.03.009.
19. Rojalin T, Kurki L, Laaksonen T, Viitala T, Kostamovaara J, Gordon KC, Galvis L, Wachsmann-Hogiu S, Strachan CJ, Yliperttula M. Fluorescence-suppressed time-resolved Raman spectroscopy of pharmaceuticals using complementary metal-oxide semiconductor (CMOS) single-photon avalanche diode (SPAD) detector. Anal Bioanal Chem. 2016;408(3):761–74. https://doi.org/10.1007/s00216-015-9156-6.
20. Wang HQ, Zhao JH, Lee AMD, Lui H, Zeng HS. Improving skin Raman spectral quality by fluorescence photobleaching. Photodiagnosis Photodyn Ther. 2012;9(4):299–302. https://doi.org/10.1016/j.pdpdt.2012.02.001.
21. Matousek P, Towrie M, Parker AW. Fluorescence background suppression in Raman spectroscopy using combined Kerr gated and shifted excitation Raman difference techniques. J Raman Spectrosc. 2002;33(4):238–42. https://doi.org/10.1002/jrs.840.
22. Le Ru EC, Schroeter LC, Etchegoin PG. Direct measurement of resonance Raman spectra and cross sections by a polarization difference technique. Anal Chem. 2012;84(11):5074–9. https://doi.org/10.1021/ac300763q.
23. Cloutis E, Szymanski P, Applin D, Goltz D. Identification and discrimination of polycyclic aromatic hydrocarbons using Raman spectroscopy. Icar. 2016;274:211–30. https://doi.org/10.1016/j.icarus.2016.03.023.
24. Kaszowska Z, Malek K, Staniszewska-Slezak E, Niedzielska K. Raman scattering or fluorescence emission? Raman spectroscopy study on lime-based building and conservation materials.

Spectrochim Acta A Mol Biomol Spectrosc. 2016;169:7–15. https://doi.org/10.1016/j.saa.2016.06.012.
25. Zhao J, Carrabba MM, Allen FS. Automated fluorescence rejection using shifted excitation Raman difference spectroscopy. Appl Spectrosc. 2002;56(7):834–45. https://doi.org/10.1366/000370202760171491.
26. De Luca AC, Mazilu M, Riches A, Herrington CS, Dholakia K. Online fluorescence suppression in modulated Raman spectroscopy. Anal Chem. 2009;82(2):738–45. https://doi.org/10.1021/ac9026737.
27. Gebrekidan MT, Knipfer C, Stelzle F, Popp J, Will S, Braeuer A. A shifted-excitation Raman difference spectroscopy (SERDS) evaluation strategy for the efficient isolation of Raman spectra from extreme fluorescence interference. J Raman Spectrosc. 2016;47(2):198–209. https://doi.org/10.1002/jrs.4775.
28. Lin J, Lin D, Qiu S, Huang Z, Liu F, Huang W, Xu Y, Zhang X, Feng S. Shifted-excitation Raman difference spectroscopy for improving in vivo detection of nasopharyngeal carcinoma. Talanta. 2023;257. https://doi.org/10.1016/j.talanta.2023.124330.
29. Sowoidnich K, Maiwald M, Ostermann M, Sumpf B. Shifted excitation Raman difference spectroscopy for soil component identification and soil carbonate determination in the presence of strong fluorescence interference. J Raman Spectrosc. 2023;54(11):1327–40. https://doi.org/10.1002/jrs.6500.
30. Mosier-Boss P, Lieberman S, Newbery R. Fluorescence rejection in Raman spectroscopy by shifted-spectra, edge detection, and FFT filtering techniques. Appl Spectrosc. 1995;49(5):630–8.
31. Cai WS, Wang LY, Pan ZX, Zuo J, Xu CY, Shao XG. Application of the wavelet transform method in quantitative analysis of Raman spectra. J Raman Spectrosc. 2001;32(3):207–9. https://doi.org/10.1002/jrs.688.
32. Tan HW, Brown SD. Wavelet analysis applied to removing non-constant, varying spectroscopic background in multivariate calibration. J Chemom. 2002;16(5):228–40. https://doi.org/10.1002/cem.717.
33. Lieber CA, Mahadevan-Jansen A. Automated method for subtraction of fluorescence from biological Raman spectra. Appl Spectrosc. 2003;57(11):1363–7. https://doi.org/10.1366/00037020332255451 8.
34. Cao A, Pandya AK, Serhatkulu GK, Weber RE, Dai H, Thakur JS, Naik VM, Naik R, Auner GW, Rabah R, Freeman DC. A robust method for automated background subtraction of tissue fluorescence. J Raman Spectrosc. 2007;38(9):1199–205. https://doi.org/10.1002/jrs.1753.
35. Zhao J, Lui H, McLean DI, Zeng H. Automated autofluorescence background subtraction algorithm for biomedical Raman spectroscopy. Appl Spectrosc. 2007;61(11):1225–32. https://doi.org/10.1366/000370207782597003.
36. Lin K, Zhou XG, Liu SL, Luo Y. Identification of free OH and its implication on structural changes of liquid water. Chin J Chem Phys. 2013;26(2):121–6. https://doi.org/10.1063/1674-0068/26/02/121-126.
37. Tang CQ, Lin K, Zhou XG, Liu SL. Detection of amide A bands of proteins in water by Raman spectrum. Chin J Chem Phys. 2016;29(1):129–34. https://doi.org/10.1063/1674-0068/29/cjcp1511240.
38. Wang YX, Zhu WD, Lin K, Yuan LF, Zhou XG, Liu SL. Ratiometric detection of Raman hydration shell spectra. J Raman Spectrosc. 2016;47(10):1231–8. https://doi.org/10.1002/jrs.4940.
39. Wang Z, Ju S, Wang Y, Zhang R, Ma L, Song J, Lin K. The isosbestic point in the Raman spectra of the hydration shell. Spectrochim Acta A Mol Biomol Spectrosc. 2024;317:124413. https://doi.org/10.1016/j.saa.2024.124413.
40. Jin Z, Kong X, Wang Z, Zhang R, Ma L, Lin K. Solvent shared ion pairs and direct contacted ion pairs in LiCl aqueous solution by IR ratio spectra. J Solution Chem. 2023. https://doi.org/10.1007/s10953-023-01339-3.
41. Wang Z, Duan S, Fang B, Liu Z, Zhang R, Ma L, Lin K. Identification of the molecular structure of mandelic acid in solid and aqueous solutions by Raman spectra in the C-H/C-D stretching region. Vib Spectrosc. 2022;120. https://doi.org/10.1016/j.vibspec.2022.103382.
42. Rajasekar M. Recent trends in rhodamine derivatives as fluorescent probes for biomaterial applications. J Mol Struct. 2021;1235. https://doi.org/10.1016/j.molstruc.2021.130232.
43. Basuri P, Shantha Kumar J, Unni K, Manna S, Pradeep T. Aggregation of molecules is controlled in microdroplets. Chem Commun. 2022;58(91):12657–60. https://doi.org/10.1039/d2cc04587g.
44. Shafer-Peltier KE, Haka AS, Fitzmaurice M, Crowe J, Myles J, Dasari RR, Feld MS. Raman microspectroscopic model of human breast tissue: implications for breast cancer diagnosis. J Raman Spectrosc. 2002;33(7):552–63. https://doi.org/10.1002/jrs.877.
45. Haka AS, Shafer-Peltier KE, Fitzmaurice M, Crowe J, Dasari RR, Feld MS. Diagnosing breast cancer by using Raman spectroscopy. Proc Natl Acad Sci U S A. 2005;102(35):12371–6. https://doi.org/10.1073/pnas.0501390102.
46. Haka AS, Volynskaya Z, Gardecki JA, Nazemi J, Lyons J, Hicks D, Fitzmaurice M, Dasari RR, Crowe JP, Feld MS. Margin assessment during partial mastectomy breast surgery using Raman spectroscopy. Cancer Res. 2006;66(6):3317–22. https://doi.org/10.1158/0008-5472.CAn-05-2815.
47. Zehentbauer FM, Moretto C, Stephen R, Thevar T, Gilchrist JR, Pokrajac D, Richard KL, Kiefer J. Fluorescence spectroscopy of Rhodamine 6G: concentration and solvent effects. Spectrochim Acta Part A Mol Biomolecul Spectrosc. 2014;121:147–51. https://doi.org/10.1016/j.saa.2013.10.062.
48. Picard A, Daniel I, Montagnac G, Oger P. In situ monitoring by quantitative Raman spectroscopy of alcoholic fermentation by under high pressure. Extremophiles. 2007;11(3):445–52. https://doi.org/10.1007/s00792-006-0054-x.
49. Kiefer J, Toni F, Wirth KE. Influence of carbon-coated iron nanoparticles on the Raman spectrum of liquid ethanol. J Raman Spectrosc. 2015;46(11):1124–8. https://doi.org/10.1002/jrs.4743.
50. Safir F, Vu N, Tadesse LF, Firouzi K, Banaei N, Jeffrey SS, Saleh AAE, Khuri-Yakub BT, Dionne JA. Combining acoustic bioprinting with AI-assisted Raman spectroscopy for high-throughput identification of bacteria in blood. Nano Lett. 2023;23(6):2065–73. https://doi.org/10.1021/acs.nanolett.2c03015.
51. Arend N, Pittner A, Ramoji A, Mondol AS, Dahms M, Rüger J, Kurzai O, Schie IW, Bauer M, Popp J, Neugebauer U. Detection and differentiation of bacterial and fungal infection of neutrophils from peripheral blood using Raman spectroscopy. Anal Chem. 2020;92(15):10560–8. https://doi.org/10.1021/acs.analchem.0c01384.
52. Movasaghi Z, Rehman S, Rehman IU. Raman spectroscopy of biological tissues. Appl Spectrosc Rev. 2007;42(5):493–541. https://doi.org/10.1080/05704920701551530.

Zhiqiang Wang is a lecturer in the School of Physics in Xidian University. He received his doctor's degree from Dalian Institute of Chemical Physics, Chinese Academy of Sciences. His major interests focus on developing novel spectroscopic methods to study intermolecular interactions and surface photochemical reactions.

Siwen Ju received her master's degree from Xidian University. Her major interests focus on developing new methods for Raman spectroscopy to study the local structure of aqueous solutions and intermolecular interactions.

Xiaofei Zhou is currently working as Deputy Chief Technician in the Affiliated Hospital of Xidian University. She received her bachelor's degree from Northwest University. In recent years, she has been interested in using new methods for medical laboratory work.

Feng Ni received his master's degree from Xi'an Jiaotong University. He is now Chief Physician of the Urology Department at the Third Affiliated Hospital of Xi'an Medical College. He is mainly engaged in the diagnosis and treatment of cancer of the urinary system, and research on the combination of medical and industrial technology.

Yanhua Qiu is currently working as a doctor in the Affiliated Hospital of Xidian University. She received her bachelor's degree from Wannan Medical College. Her current interests are in the use of novel techniques for the treatment of common gynecological diseases and gynecological oncology.

Ruiting Zhang received his doctor's degree from the University of Science and Technology of China. He is now Associate Professor at the School of Physics, Xidian University. He is mainly engaged in theoretical and computational spectroscopy.

Lin Ma received her PhD degree from Xian Jiaotong University in 2016. Currently, she is working as Associate Professor at the School of Physics, Xidian University. She mainly focuses on first-principles calculations of photoelectric functional materials.

Ke Lin is Associate Professor in the School of Physics at Xidian University. He received his doctor's degree from the University of Science and Technology of China. His current interests focus on developing novel Raman and IR spectroscopy to study the local structure of aqueous solutions, intermolecular interactions, and the safety of foods.